Impact of plant water uptake strategy on soil moisture and evapotranspiration dynamics during drydown

Adriaan J. Teuling,[1] Remko Uijlenhoet,[1] François Hupet,[2] and Peter A. Troch[1]

Received 21 October 2005; revised 28 November 2005; accepted 5 December 2005; published 2 February 2006.

[1] Experiments have shown that plants can compensate for water stress in the upper, more densely rooted, soil layers by increasing the water uptake from deeper layers. By adapting root water uptake to water availability, plants are able to extend the period of unstressed transpiration. This strategy conflicts with the approach in many land surface schemes, where plant water uptake is treated as a static process. Here we derive expressions for the typical drydown trajectories of evapotranspiration and soil moisture for both strategies. We show that the maximum difference in evapotranspiration between the two strategies during drydown can exceed 50%. This in turn leads to a difference in root zone soil moisture of up to 25%. The results stress the importance of incorporating realistic root water uptake concepts in land surface schemes.
Citation: Teuling, A. J., R. Uijlenhoet, F. Hupet, and P. A. Troch (2006), Impact of plant water uptake strategy on soil moisture and evapotranspiration dynamics during drydown, *Geophys. Res. Lett.*, *33*, L03401, doi:10.1029/2005GL025019.

1. Introduction

[2] Climate model simulations are sensitive to root water uptake parameters in their land surface schemes [*Desborough*, 1997; *Milly*, 1997; *Kleidon and Heimann*, 1998; *Zeng et al.*, 1998]. A correct parameterization of the root water uptake (hereafter RWU) process is essential to predict the long-term (multiple day to monthly) evolution of energy flux partitioning at the land surface. At seasonal timescales, perennial vegetation is known to adapt its root pattern to the availability of soil moisture [*Nepstad et al.*, 1994; *Wan et al.*, 2002]. At much shorter timescales (multiple days to weeks), there is also evidence that (non-drought adapted) annual vegetation has strategies to cope with water shortage in (the upper) part of the soil. This often results in water extraction from deeper layers at rates much higher than would be expected on the basis of the root density [*Sharp and Davies*, 1985; *Green and Clothier*, 1995]. By doing so, plants are able to delay loss of turgor, prevent stomatal closure, and maintain a high rate of photosynthesis. Rather than by a complete adjustment of the root density profile, plants adapt to drought by rapidly developing fine roots [*Coelho and Or*, 1999], or by increasing the activity and efficiency of deep roots [*Sharp and Davies*, 1985]. Deep roots can be responsible for the bulk of the water uptake [*Lai and Katul*, 2000].

[3] Several algorithms have been developed that can compensate for water stress in part of the root zone by allowing increased uptake from other parts [*Hoogland et al.*, 1981; *Jarvis*, 1989; *Adiku et al.*, 2000; *Li et al.*, 2001]. These algorithms allow for a longer period of unstressed transpiration, without altering the rooting depth or the available soil moisture. In this paper we investigate the potential impact of the RWU strategy on the coupled dynamics of soil moisture and evapotranspiration during drydown for the simplified case where root water uptake dominates other flow mechanisms. We distinguish between a static strategy (hereafter referred to as S), where RWU is driven by local conditions, and an adaptive strategy (A), where RWU also depends on root zone average soil moisture conditions.

2. Modeling Root Water Uptake

[4] The water budget in the root zone is described by:

$$\frac{\partial \theta}{\partial t} = -\frac{\partial q}{\partial z} - S \tag{1}$$

where θ is the volumetric soil moisture content, z a vertical coordinate (positive downwards), q the vertical moisture flux, and S a sink term representing RWU. Land surface modelers often adopt strategy S and assume that RWU is proportional to a maximum (unstressed) evapotranspiration rate E_m, the root density distribution p_r, and a water stress factor β [*Feddes et al.*, 2001]. For many plants, root density is highest near the land surface and decays exponentially with depth [*Gerwitz and Page*, 1974]. For practical reasons we use the apparent root density distribution $p_r^*(z)$ defined over the effective rooting depth L:

$$p_r^*(z) = \lambda' e^{-\lambda z} \tag{2}$$

where λ is the inverse of the e-folding depth of the root density, and $\lambda' = \lambda/(1 - e^{-\lambda L})$ such that $\int_0^L p_r^*(z)\,\mathrm{d}z = 1$. We assume the e-folding depth of the root density and the effective rooting depth to be related, i.e. $L = c/\lambda$. If L is taken as the depth in (2) above which 95% of the roots are found [e.g. *Schenk and Jackson*, 2002], then $c \approx 3$. Water stress can be modeled as a piecewise linear function of θ:

$$\beta(\theta) = \begin{cases} 0, & \theta \le \theta_w \\ \dfrac{\theta - \theta_w}{\theta_c - \theta_w}, & \theta_w < \theta \le \theta_c \\ 1, & \theta_c < \theta \le \theta_s \end{cases} \tag{3}$$

[1]Hydrology and Quantitative Water Management Group, Wageningen University, Wageningen, Netherlands.
[2]Department of Environmental Sciences and Land Use Planning, Université Catholique de Louvain, Louvain-la-Neuve, Belgium.

Copyright 2006 by the American Geophysical Union.
0094-8276/06/2005GL025019$05.00

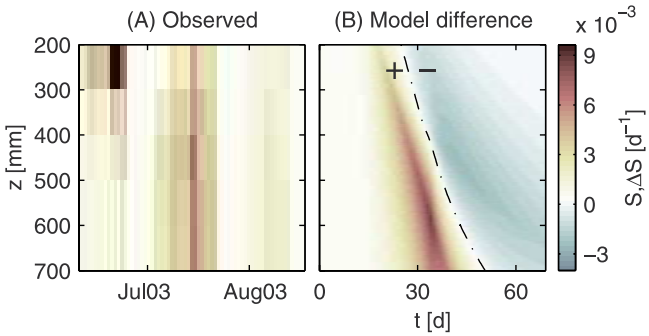

Figure 1. Root water uptake (S) in an experimental field in Louvain-la-Neuve, Belgium. (A) Observed. (B) Model difference ΔS between the algorithm of *Jarvis* [1989] and $S = E_m\beta(\theta)p_r^*(z)$, using E_m = 4 mm d^{-1}, λ = 3 m^{-1}, θ_w = 0.16, θ_c = 0.22, θ_0 = 0.35, and a critical value of the weighted stress index of 0.2.

where θ_s is the moisture content at saturation, θ_c the critical moisture level, and θ_w the wilting point. When $\partial q/\partial z \ll S$ (as is typical under dry conditions), the local soil moisture decay can be obtained by solving $\partial\theta(z, t)/\partial t = -E_m\beta(\theta)p_r^*(z)$. Starting from a (uniform) initial soil moisture content θ_0 at $t = 0$ with $\theta_0 > \theta_c$, this yields the following expression for $\theta(z, t)$ at a daily timescale:

$$\theta'(z,t) = \begin{cases} \theta_0' - \lambda' e^{-\lambda z} E_m t, & 0 \le t < t_c(z) \\ \theta_c' \exp\left(\dfrac{\theta_0' - \theta_c'}{\theta_c'} - \dfrac{\lambda' e^{-\lambda z} E_m t}{\theta_c'}\right), & t \ge t_c(z). \end{cases} \tag{4}$$

where $t_c(z)$ relates the time t_c and corresponding depth z_c of the first reduction on S ($\theta'(z, t) = \theta_c$):

$$t_c(z) = \frac{\theta_0' - \theta_c'}{E_m \lambda' \exp(-\lambda z)} \Leftrightarrow z_c(t) = \frac{1}{\lambda}\log\left(\frac{E_m \lambda' t}{\theta_0' - \theta_c'}\right) \tag{5}$$

and θ' denotes the transformed variable $\theta' = \theta - \theta_w$.

[5] For strategy A algorithms, an expression for $\theta'(z, t)$ will also depend on the co-evolution of the root zone averaged soil moisture $\bar{\theta}(t)$ [*Jarvis*, 1989]. Since our interest is in the total (depth integrated) RWU rather than $\theta'(z, t)$, we assume that the total RWU response for strategy A algorithms is similar to (3) evaluated directly with $\bar{\theta}$, i.e. with stress $\beta(\bar{\theta})$. The validity of this assumption increases with the plants ability to compensate for stress [e.g. *Guswa et al.*, 2002]. Since the onset of reduced RWU occurs at min[$t_c(z)$] or at max[$p_r^*(z)$], it can be seen from (5) that strategy A (single reservoir with effective uniform p_r) tends to maximize t_c. In this way, the onset of water stress is postponed, but at the risk of more severe stress at a later stage.

3. A Field Example

[6] Figure 1A shows the RWU as derived from successive soil moisture measurements during periods without significant rainfall made in a field cropped with maize (*Zea mays* L.) in Louvain-la-Neuve (Belgium) during the 2003 European heat wave [*Hupet and Vanclooster*, 2005]. During the initial stage of drying (June), the higher RWU in the upper part of the profile mimics the exponential root density profile. During the second stage (mid July), the bulk of the RWU shifted downwards due to drying of the topsoil. Moreover, the rate of water uptake at these depths was fourfold that of the previous period, indicating a transition of RWU from root distribution-controlled towards water availability-controlled [*Green and Clothier*, 1995]. In August the uptake at all measured depths was low.

[7] To illustrate the effect of RWU parameterization on the simulation of similar events, Figure 1b shows the difference in RWU between a numerical evaluation of the *Jarvis* [1989] algorithm with stress compensation (strategy A) and without compensation (strategy S). The parameters were chosen to match the conditions at the site and vertical flow was neglected. Initially, both models give identical results. However, large differences occur for $t > 25$ d when reduced uptake in the upper part of the soil for strategy S is compensated by higher uptake rates at larger depths for strategy A. Interestingly, both the depth and timing of these differences are similar to the increased uptake in Figure 1A. Later, the differences switch sign, but are of smaller magnitude. This example shows that models based on strategy S might fail to capture the actual RWU dynamics. The timescales where the differences are large are highly relevant to many land surface forecast problems.

4. Evapotranspiration Decay

[8] The total RWU for strategy S is obtained by integrating $S(z, t)$ over the profile (denoted by $\widehat{S}$), while accounting for vertical differences in soil moisture reduction:

$$\widehat{S}_S(t) = \begin{cases} \lambda' E_m \displaystyle\int_0^L e^{-\lambda z}\mathrm{d}z = E_m, \\ 0 \le t < t_c(0) \\ \lambda' E_m \displaystyle\int_0^{z_c} \frac{\theta'(z,t)}{\theta_c'} e^{-\lambda z}\mathrm{d}z + \lambda' E_m \int_{z_c}^L e^{-\lambda z}\mathrm{d}z, \\ t_c(0) \le t < t_c(L) \\ \lambda' E_m \displaystyle\int_0^L \frac{\theta'(z,t)}{\theta_c'} e^{-\lambda z}\mathrm{d}z, \\ t \ge t_c(L). \end{cases} \tag{6}$$

where $z_c(t)$ is given by (5). Integration of (6) with substitution of $z_c(t)$ and (4), and rearranging of the different terms yields:

$$\sigma_S(\tau) = \begin{cases} 1, \\ 0 \le \tau < \dfrac{1-f}{b} \\ \dfrac{1}{\tau} - \dfrac{f}{\tau}\exp\left(\dfrac{1-f}{f} - \dfrac{b\tau}{f}\right) - be^{-c}, \\ \dfrac{1-f}{b} \le \tau < \dfrac{1-f}{be^{-c}} \\ \dfrac{f}{\tau}\exp\left(\dfrac{1-f}{f}\right)\left[\exp\left(-\dfrac{b\tau}{f}e^{-c}\right) - \exp\left(-\dfrac{b\tau}{f}\right)\right], \\ \tau \ge \dfrac{1-f}{be^{-c}} \end{cases} \tag{7}$$

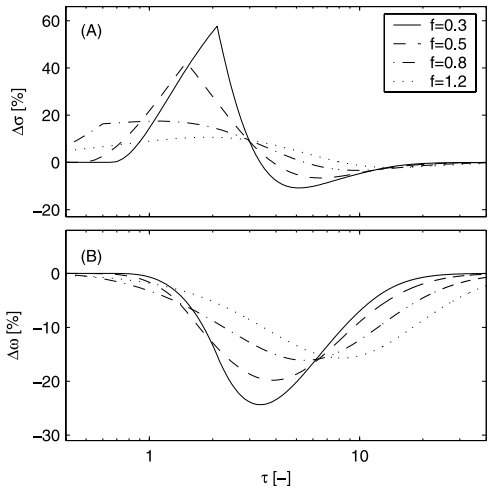

Figure 2. Relative impact of uptake strategy on (A) evaporative flux σ and (B) soil moisture ω as a function of normalized time $\tau = \lambda E_m t/\theta'_0$, for different *f*.

where the dimensionless variables $\sigma = \widehat{S}/E_m$, $f = \theta'_c/\theta'_0$, $b = \lambda'/\lambda$, and $\tau = \lambda E_m t/\theta'_0$ have been introduced for convenience. If $\theta_0 \leq \theta_c$ ($f \geq 1$), the solution reduces to:

$$\sigma_S(\tau) = \frac{1}{\tau}\left[\exp\left(-\frac{b\tau}{f}e^{-c}\right) - \exp\left(-\frac{b\tau}{f}\right)\right] \tag{8}$$

[9] For strategy A, the time to first reduction on RWU becomes: $t_c = L(\theta'_0 - \theta'_c)/E_m$, or $\tau_c = c - cf$. By using $\overline{\theta}$ rather than θ in (3), the time evolution of σ_A can be written as:

$$\sigma_A(\tau) = \begin{cases} 1, & 0 \leq \tau < c - cf \\ \exp\left(\frac{1-f}{f} - \frac{\tau}{cf}\right), & \tau \geq c - cf \end{cases} \tag{9}$$

[10] We define the relative difference Δσ at time $\tau = \tau^*$ between strategy A and S as: $\Delta\sigma|_{\tau=\tau^*} = \sigma_A(\tau^*) - \sigma_S(\tau^*)$. The maximum difference max(|Δσ|) occurs at the onset of reduced uptake for A. With the values used in Figure 1b, this corresponds to $t \approx 33$ d. The difference $\Delta\sigma|_{\tau=c-cf}$ can be evaluated by using $\sigma_A = 1$ and inserting $\tau = c - cf$ in (7). For Figure 1b this yields max(|Δσ|) ≈ 46%.

[11] Values for *f* depend on soil, climate, vegetation, and/or initial conditions, but are typically in the range of 0.3–0.6. In Figure 2A, Δσ(τ) is evaluated for different *f*. Strategy A initially leads to considerable higher evapotranspiration rates than strategy S with a maximum difference of over 50% for low *f*. During later stages of drydown the difference is opposite but much smaller in magnitude (see also Figure 2B). The maximum difference is strongly dependent on *f*. For $f \geq 1$, the maximum difference ($\Delta\sigma|_{\tau=c-cf}$) reduces to less than 10%.

5. Soil Moisture Decay

[12] The evolution of soil moisture averaged over a layer of thickness *L* and scaled by θ'_0, $\omega = \overline{\theta'}/\theta'_0$, can be derived from (4) by separating between non-, partly-, and fully reduced RWU trajectories similar to (6). For strategy S this yields:

$$\omega_S(\tau) = \begin{cases} 1 - \frac{\tau}{c}, \\ 0 \leq \tau < \frac{1-f}{b} \\ 1 + \frac{b\tau}{c}e^{-c} + \frac{1}{c}\log\left(\frac{1-f}{b\tau}\right) + \frac{f-1}{c} \\ +\frac{f}{c}\exp\left(\frac{1-f}{f}\right)\left[\mathrm{E}_1\left(\frac{1-f}{f}\right) - \mathrm{E}_1\left(\frac{b\tau}{f}\right)\right], \\ \qquad \frac{1-f}{b} \leq \tau < \frac{1-f}{be^{-c}} \\ \frac{f}{c}\exp\left(\frac{1-f}{f}\right)\left[\mathrm{E}_1\left(\frac{b\tau}{f}e^{-c}\right) - \mathrm{E}_1\left(\frac{b\tau}{f}\right)\right], \\ \tau \geq \frac{1-f}{be^{-c}}. \end{cases} \tag{10}$$

where E_1 is the exponential integral. For $\theta_0 \leq \theta_c$ the solution reduces to:

$$\omega_S(\tau) = \frac{1}{c}\left[\mathrm{E}_1\left(\frac{b\tau}{f}e^{-c}\right) - \mathrm{E}_1\left(\frac{b\tau}{f}\right)\right] \tag{11}$$

[13] Similarly, the normalized soil moisture evolution for strategy A for $\theta_0 > \theta_c$ is given by:

$$\omega_A(\tau) = \begin{cases} 1 - \frac{\tau}{c}, & 0 \leq \tau < c - cf \\ f\exp\left(\frac{1-f}{f} - \frac{\tau}{cf}\right), & \tau \geq c - cf. \end{cases} \tag{12}$$

which is similar to (4). We define Δω as the difference in transformed and normalized soil moisture between strategy A and S: $\Delta\omega|_{\tau=\tau^*} = \omega_A(\tau^*) - \omega_S(\tau^*)$. Evaluation of Δω(τ) in Figure 2b shows that strategy A systematically leads to lower values of the available root zone soil moisture during drydown when compared to strategy S. This is caused by the faster soil-controlled limitation on $\widehat{S}_S$ and associated lower $d\overline{\theta}_S/dt$. The maximum difference for low values of *f* is

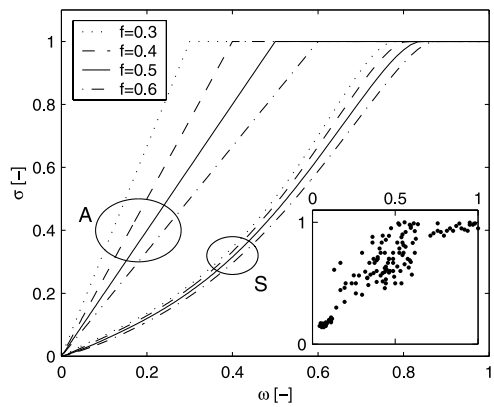

Figure 3. Scaled relationships between root water uptake and root zone average soil moisture for static (S) and adaptive (A) RWU and different values of *f* during drydown. Inset: lysimeter observations made by *Homaee et al.* [2002] on alfalfa (*Medicago Sativa* L.) with *L* = 0.6 m.

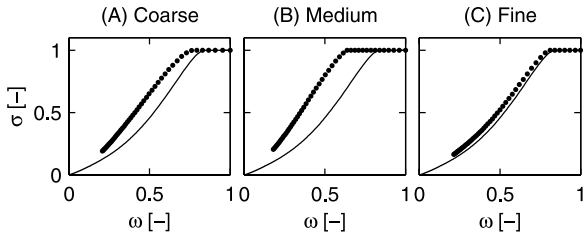

Figure 4. Relation between daily σ and ω for strategy S (f = 0.5) for a Richards' equation-based model (dots, E_m = 4 mm d^{-1}, λ = 3 m^{-1}), and the analytical model (7) and (10) without vertical flow (curves). (A) Coarse, (B) Medium, and (C) Fine soil.

in the order of 25%. Since soil moisture reflects the effect of preceding RWU, the maximum difference in Δω lags behind the maximum difference in Δσ. With the values used in Figure 1b, the maximum Δω occurs at $t \approx 53$ d. These timescales are especially relevant in the context of seasonal forecasting. Since for both strategies soil moisture is integrated over the same layer, Δω = 0 for $\tau \rightarrow \infty$. Although the maximum of $\Delta\sigma|_{\tau=\tau^*}$ is strongly reduced for large f, this reduction is less pronounced in the integrated effect on $\Delta\omega|_{\tau=\tau^*}$. Here the maximum absolute difference only shows a slight reduction for high f.

6. Root Zone Aggregation

[14] It is also interesting to study the effect of uptake strategy on the relation between soil moisture and evaporation aggregated over the root zone. Figure 3 shows the drydown trajectories plotted in the ω, σ-domain for different f (0.3–0.6). The curves for strategy S reveal little sensitivity to f. For small f, the difference in evaporative flux between the two strategies at a given value of ω, $\Delta\sigma|_{\omega=\omega^*}$, can exceed $\Delta\sigma|_{\tau=\tau^*}$. The difference is largest for $\bar{\theta} = \theta_c$ ($\omega = f$). $\Delta\sigma|_{\omega=f}$ easily exceeds 50% for low f. Figure 3 shows that even when reliable estimates of root zone soil moisture are available, estimates of actual evapotranspiration can be highly uncertain due to a wrong RWU conceptualization, and vice versa. Differences in the aggregated ω, σ-relation resulting from differences in compensation ability were also reported by [*Guswa et al.*, 2002].

[15] The inset in Figure 3 shows an example of the observed relation between ω and σ [*Homaee et al.*, 2002]. The piecewise linear behavior ($f \approx 0.5$) is typical for many other similar experiments. Since the curves serve as an upper envelope for the measurements, they are best characterized by strategy A (see also Figure 1). Only few points fall below the curves for strategy S.

[16] To test whether our results are dependent on the assumption of no vertical moisture transport, we performed drydown simulations with a Richards' equation based model with RWU according to strategy S (by definition, the results for strategy A are trivial). θ_0 was set as the average soil moisture after 3 days of free drainage starting from saturation. Figure 4 shows that for typical coarse and fine soils the results closely match the curve without vertical flow. For medium textured soils, redistribution has a compensating effect on vertical differences in RWU, so that maximum RWU can be sustained at lower $\bar{\theta}$. The results will converge towards our analytical model for lower θ_0 (through its strong nonlinear effect on conductivity) or λ (through smaller gradients). Also the occurrence of rainfall events will influence our results for strategy S by their influence on the vertical soil moisture distribution. The associated hysteresis effects that arise from partial rewetting of the soil profile are discussed by *Guswa* [2005].

7. Discussion and Conclusion

[17] In this paper we show that different RWU strategies can lead to large differences in the temporal evolution of evapotranspiration and soil moisture during drydown, even when the available soil moisture is left unaltered. We find that, in absence of vertical flow, these differences can be as high as 50% for evapotranspiration and 25% for soil moisture. The compensating effect of vertical flow in the soil profile depends on several factors, but is likely to be minor for most realistic conditions. We find that even for a relatively high initial soil moisture content, the assumption of no vertical flow is reasonable for coarse and fine soils. Our results suggest that land surface schemes with a realistic (static) root distribution but no stress compensation underestimate the actual RWU in water-limited conditions. The timescales at which the largest differences occur (multiple weeks) are highly relevant for drought forecasting. A better representation of RWU processes in land surface schemes could help to improve their predictive capability under these conditions.

[18] **Acknowledgments.** We thank Mehdi Homaee for sharing his data with us. This research is supported by the Wageningen Institute for Environment and Climate Research (WIMEK) and the project Development of a European Land Data Assimilation System to predict Floods and Droughts (ELDAS, EVG1-CT-2001-00050). R.U. acknowledges financial support from the Netherlands Organization for Scientific Research (NWO) through a Innovational Research Incentives Scheme grant (Project 016.021.003).

References

Adiku, S., C. Rose, R. Braddock, and H. Ozier-Lafontaine (2000), On the simulation of root water extraction: Examination of a minimum energy hypothesis, *Soil Sci.*, *165*(3), 226–236.

Coelho, E., and D. Or (1999), Root distribution and water uptake patterns of corn under surface and subsurface drip irrigation, *Plant Soil*, *206*(2), 123–136.

Desborough, C. (1997), The impact of root weighting on the response of transpiration to moisture stress in land surface schemes, *Mon. Weather Rev.*, *125*(8), 1920–1930.

Feddes, R., et al. (2001), Modeling root water uptake in hydrological and climate models, *Bull. Am. Meteorol. Soc.*, *82*(12), 2797–2809.

Gerwitz, A., and E. Page (1974), An empirical mathematical model to describe plant root systems, *J. Appl. Ecol.*, *11*(2), 773–781.

Green, S., and B. Clothier (1995), Root water uptake by kiwifruit vines following partial wetting of the root zone, *Plant Soil*, *173*, 317–328.

Guswa, A. (2005), Soil-moisture limits on plant uptake: An upscaled relationship for water-limited ecosystems, *Adv. Water Resour.*, *28*, doi:10.1016/j.advwatres.2004.08.016.

Guswa, A., M. Celia, and I. Rodriguez-Iturbe (2002), Models of soil moisture dynamics in ecohydrology: A comparative study, *Water Resour. Res.*, *38*(9), 1166, doi:10.1029/2001WR000826.

Homaee, M., R. Feddes, and C. Dirksen (2002), Simulation of root water uptake II. Non-uniform transient water stress using different reduction functions, *Agric. Wat. Mngt.*, *57*, 111–126.

Hoogland, J., R. Feddes, and C. Belmans (1981), Root water uptake model depending on soil water pressure head and maximum extraction rate, *III International Symposium on Water Supply and Irrigation in the Open and Under Protected Cultivation*, *ISHS Acta Hortcult.*, *119*, edited by W. A. Wagenvoort, 123–136, Leuven, Belgium.

Hupet, F., and M. Vanclooster (2005), Micro-variability of hydrological processes at the maize row scale: Implications for soil water content

measurements and evapotranspiration estimates, *J. Hydrol.*, *303*, 247–270, doi:10.1016/j.jhydrol.2004.07.017.

Jarvis, N. (1989), A simple empirical model of root water uptake, *J. Hydrol.*, *107*, 57–72.

Kleidon, A., and M. Heimann (1998), Optimised rooting depth and its impacts on the simulated climate of an Atmospheric General Circulation Model, *Geophys. Res. Lett.*, *25*(3), 345–348.

Lai, C., and G. Katul (2000), The dynamic role of root-water uptake in coupling potential to actual transpiration, *Adv. Water Resour.*, *23*(4), 427–439.

Li, K., R. De Jong, and J. Boisvert (2001), An exponential root-water-uptake model with water stress compensation, *J. Hydrol.*, *252*, 189–204.

Milly, P. (1997), Sensitivity of greenhouse summer dryness to changes in plant rooting characteristics, *Geophys. Res. Lett.*, *24*(3), 269–271.

Nepstad, D., et al. (1994), The role of deep roots in the hydrological and carbon cycles of Amazonian forests and pastures, *Nature*, *372*(6507), 666–669.

Schenk, H., and R. Jackson (2002), The global biogeography of roots, *Ecol. Monogr.*, *72*(3), 311–328.

Sharp, R., and W. Davies (1985), Root growth and water uptake by maize plants in drying soil, *J. Exp. Bot.*, *36*(170), 1441–1456.

Wan, C., I. Yilmaz, and R. Sosebee (2002), Seasonal soil-water availability influences snakeweed root dynamics, *J. Arid Environ.*, *51*, 255–264, doi:10.1016/jare.2001.0942.

Zeng, X., Y. Dai, R. Dickinson, and M. Shaikh (1998), The role of root distribution for climate simulation over land, *Geophys. Res. Lett.*, *25*(24), 4533–4536.

F. Hupet, Department of Environmental Sciences and Land Use Planning, Université Catholique de Louvain, B-1348 Louvain-la-Neuve, Belgium.

A. J. Teuling, P. A. Troch, and R. Uijlenhoet, Hydrology and Quantitative Water Management Group, Wageningen University, Nieuwe Kanaal 11, NL-6709 PA Wageningen, Netherlands. (ryan.teuling@wur.nl)